Charge exchange and excitation in Ne^{+}/a:Si collision at medium energy (2-30 keV). Experiment and simulation

1998 J. Phys.: Condens. Matter 10 8629

(http://iopscience.iop.org/0953-8984/10/39/002)

J. Phys.: Condens. Matter **10** (1998) 8629–8641. Printed in the UK PII: S0953-8984(98)89732-4

Charge exchange and excitation in Ne^+/a:Si collision at medium energy (2–30 keV). Experiment and simulation

S Mouhammad, P Benoit-Cattin†, C Benazeth, P Cafarelli, P Reynes, M Richard-Viard and J P Ziesel

Laboratoire Collisions Agrégats Réactivité (UMR 5589-CNRS), Université Paul Sabatier, 31062 Toulouse Cedex, France

Received 2 December 1997, in final form 18 May 1998

Abstract. Ne^+ ions were scattered from an amorphous silicon surface (a:Si) at relatively low incident energy (2–30 keV) to investigate the charge exchange processes and the electronic excitation mechanisms. The study was carried out as a function of several experimental parameters: primary energy (E_0), incidence angle (α) and scattering angle (θ). We show in this study that neutralization in the subsurface region of Si plays a significant role. The electron spectra show the same predominant Ne^{**} autoionizing peaks as observed in scattering from metallic surfaces and the core rearrangement mechanisms used for explaining the $^1D \rightarrow {}^3P$ conversion are still valid. The conversion efficiency is an increasing function of the incidence angle and a decreasing one of the beam energy in the 1–5 keV range; however this efficiency remains nearly constant at higher energies. This behaviour is attributed to a direct production of Ne^{**} states not assisted by core rearrangement processes.

1. Introduction

During the scattering of noble gas ions from solid surfaces, important processes of charge exchange may occur between the electron cloud of the impinging particle and the electron valence band of the surface. The interaction with the surface is often described by dividing projectile trajectory into three parts: the incoming trajectory, the close encounter and the outgoing trajectory. Following Hagstrum [1] it is assumed that Auger and (quasi) resonant charge transfer occur along the incoming and outgoing trajectories. In close collisions the projectile (ions or neutrals) can be excited electronically due to electron promotion mechanisms. In this paper, we present experimental results concerning the charge fraction of Ne^+ scattered from an amorphous silicon surface, in order to avoid directional effects linked to a monocrystalline surface; these results complete those from a previous study [2]. It is shown that the variation of the charge fraction with different collision parameters can be only accounted for by using a neutralization model dependent on the penetration of the incident ion inside the bulk material.

The interaction with the surface leads to the formation of Ne^{**} doubly excited states, extensively studied when scattering off metallic surfaces [3–5]. We present here measurements of the integral intensity of electronic transition due to the decay of the neon $^3P(3s^2)$ and $^1D(3s^2)$ autoionizing states induced by the interaction with silicon surface as a function of the projectile energy and incidence angle. As in the case of a metallic surface,

† Corresponding author.

0953-8984/98/398629+13$19.50

the ^{3}P peak is the most important, due to very efficient core conversion mechanisms in the vicinity of the surface [3, 4, 6], but for primary energies greater than 5 keV direct production plays an important role. Analysis of the autoionization peak profiles by considering the Doppler effect allows us to obtain information about the angular distributions of the emitting atoms and the core conversion processes [7, 8].

2. Experiment

A detailed description of the apparatus has been given elsewhere [9]. The experiments are carried out in a UHV chamber equipped with a time of flight (TOF-ISS-DRS) spectrometer and a high resolution electron spectrometer. The ions are extracted from a discharge source at an energy of 4 keV. After mass selection the beam is chopped by a 150 V square voltage applied between two deflection plates; before entering the UHV chamber it can be accelerated or decelerated between 1 and 30 keV and then focused on the target.

The measurements of charge fractions presented in this paper were performed using a TOF spectrometer movable around the target in the angular range 0–165°. The angular resolution of the detector is 1°. Two methods were used to determine charge fractions. In the first one, spectra of scattered particles (ions + neutrals) or neutrals alone are alternatively collected by electrostatic deflection of the ions at the entrance of the TOF line. Ion spectrum is then obtained by subtraction of the two spectra. A second method consists in accelerating the ions by applying a negative voltage on a part of the flight tube and so modifying their time of flight. This method allows measurements of very small charge fractions but, because of focusing effects, it was necessary to calibrate it with respect to the first one. Time of flight resolution, essentially due to the incident ion pulse time width, is about 30 ns.

Electron spectra were obtained with a 180° hemispherical spectrometer at the fixed angle of 90° with respect to the incident beam (angular resolution around 2° and energy resolution $\Delta E/E$ better than 10^{-3}).

Samples were prepared by sputtering at room temperature and with various incidence angles (down to 5° from the surface); amorphization of the crystal takes place during this procedure. Surface cleanliness was checked by TOF direct recoil spectroscopy (lack of H, C, O, ... signals) and surface flatness by angular distribution of scattered particles in grazing–specular geometry.

3. Charge fractions

3.1. Charge exchange model

Due to the large difference between the ionization potential of noble gas ions and the work function of a metal or a semiconductor target, neutralization processes are very efficient and the scattered charge fractions are generally low. However at keV energies the distance of closest approach between the projectile and a target atom can be very much smaller than the distance between lattice atoms and this binary close encounter between the (neutralized) projectile and a single target atom plays an important role through excitation and reionization of the projectile. In the case of collisions of neon on materials with close atomic numbers (Mg, Al, Si) and when a quasi-molecule is formed during a violent collision one or two 2p Ne electrons can be promoted via the 4fσ molecular orbital (MO) to excited or ionized states [10]. This process is very efficient in reionizing the projectile [3, 11, 12] and is manifested clearly through the production of Ne autoionizing states [3, 13].

The interaction of the incident particle with the target is generally divided into three steps: the incoming trajectory, the close collision and the outgoing trajectory [12, 14]. The charge fraction may be written

$$\eta^+ = f_i f_o(1 - P_N) + (1 - f_i) f_o P_I \tag{1}$$

where f_i and f_o are respectively the survival probability of an ion in the incoming and the outgoing path. P_I and P_N are the reionization and neutralization probabilities in the close collision.

Experiments with Ne^+ and Ne^0 on an Mg surface at 2 keV [4, 11] have shown that the projectiles are neutralized along the incoming trajectory; the charge state of the scattered particles depends essentially on the close encounter and on neutralization processes in the outgoing path. In the range 5–10 keV for Ne on Cu, Luitjens *et al* [15] arrived at the same conclusion.

Following Hagstrum [1], the survival probability with respect to Auger neutralization is given by

$$f_{i,o} = \exp\left(\frac{-v_c}{v_{i,o}^p}\right) \tag{2}$$

where v_c is the so called characteristic velocity proportional to the neutralization rate A, $v_{i,o}^p$ is the normal component of the particle velocity in the incoming (i) or outgoing (o) path respectively. This 'continuum model' gives a correct description of neutralization as long as the particle is outside the surface. However, if the particle penetrates inside the bulk material at closer distance to target atoms, this model fails in describing neutralization. Many authors have characterized the charge fraction in terms of a Hagstrum type expression where the characteristic velocity v_c is replaced by an 'effective velocity' v_c^*, a function of experimental parameters [16] which can be extracted from measured charge fractions:

$$v_c^*(E_0, \alpha, \theta) = -v_o^p \ln \eta^+.$$

Considering all these points, we assume that

(1) the primary ions are neutralized in the incoming trajectory ($f_i = 0$);

(2) the survival probability of an ion produced in the close encounter can be expressed in terms of a survival probability inside the solid f_{ins} times the Auger survival one in the outgoing path outside the solid f_o.

We make the additional assumption that

(3) the reionization essentially occurs during a single close collision with a probability equal to one.

To assess the value of f_{ins} we introduce a simple description of the 'bulk' neutralization: the neutralization probability is proportional to the time spent by the ion inside the solid after the close collision, that is to say, to the depth D where the close collision takes place and to the inverse of the normal component of the exit velocity v_o^p. The charge fraction, equal to the survival probability of the ion created during the close collision, is then given by the expression

$$\eta^+ = \exp\left(-\frac{\lambda D + v_c}{v_o^p}\right) \qquad (v_c^* = \lambda D + v_c) \tag{3}$$

where λ is the neutralization rate inside the material assumed to be constant. We have calculated the mean value of D by using the MARLOWE code [17] in which the collisions with an apsis less than 0.5 Å were analysed. This apsis value corresponds to the internuclear

distance where a step increase of the 4fσ molecular orbital of the Ne–Si system is observed (R Souda, private communication).

3.2. Charge fractions versus scattering angle

We have determined the charge fraction as the ratio of the quasi-single scattering (QSS) peak intensity of ions to that of the ion plus neutral peak in a TOF spectrum.

The variation of Ne^+ charge fraction versus scattering angle is shown in figure 1 for $E_0 = 4$ keV and two incidence angles 6° and 20° (with respect to the surface). For grazing incidence, $\alpha = 6°$, the penetration inside the solid is very weak so the simple Hagstrum model with a constant effective velocity should be used to fit the charge fraction. Indeed, using the most simple formula, $\eta^+ = f_0$, the agreement between calculated and experimental charge fractions turns out to be fairly good with $v_c^* = 4 \times 10^4$ m s^{-1}. This result proves the importance of Auger neutralization in the incoming trajectory and of the reionization process during the close collision. Therefore the charge fraction is determined by the probability of the close collision occurring and by the neutralization processes along the outgoing trajectory.

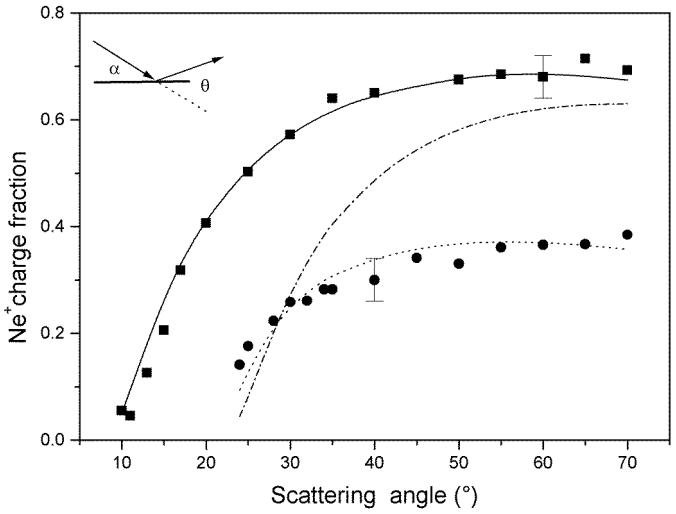

Figure 1. Variation of Ne^+ charge fraction versus scattering angle θ ($E_0 = 4$ keV) $\alpha = 6°$, ■: experimental values; ——: Hagstrum model with $v_c = 40\,000$ m s^{-1}; $\alpha = 20°$, ●: experimental values; — · —: Hagstrum model with $v_c = 40\,000$ m s^{-1}; · · · · · ·: our model (see text for numerical values).

In contrast, we found for $\alpha = 20°$ it is no longer possible to reproduce correctly the variation of the charge fraction by using the simple Hagstrum model. Because the penetration depth varies with the incidence angle, we performed a fit with expression (3) where λ and v_c are free parameters and $D(\theta)$ is given by a MARLOWE simulation. Calculations are in reasonable agreement with the measurements in the whole angular range (figure 1), with values of the free parameters being $v_c \approx 1.5 \times 10^4$ m s^{-1} and $\lambda \approx 1.8 \times 10^{14}$ s^{-1}. The value of the neutralization rate in the material (λ) is of the same order of magnitude as the Auger neutralization rates given in the literature [1, 12] $A \approx 10^{13}$–10^{15} s^{-1}. The constant value of v_c^* used in the case of $\alpha = 6°$ (4×10^4 m s^{-1}) can be split

into $v_c = 1.5 \times 10^4$ m s^{-1} and $\lambda D = 2.5 \times 10^4$ m s^{-1} corresponding to a constant value of $D = 1.4$ Å which can be attributed to the roughness of the surface and/or to the vacuum extension of the electron cloud.

3.3. Charge fractions versus incidence angle

In order to assess the role of the particle trajectory inside the solid, we performed measurements of charge fraction versus the incidence angle α at a given incident energy ($E_0 = 4$ keV) and scattering angle ($\theta = 60°$). Under these conditions, the energy of detected particles after the quasi-single scattering event is the same for all α values. It can be seen in figure 2 that the charge fraction decreases rapidly when the incidence angle increases. To check whether this is only due to the exit angle ($\theta - \alpha$) decrease of f_0 or whether neutralization inside the material occurs, we have drawn the variation of η^+, according to the simple Hagstrum model ($\eta^+ = f_0$) with $v_c^* = 4 \times 10^4$ m s^{-1} which gives the correct value of η^+ for a grazing incidence angle ($\alpha = 6°$). It is clear that the calculated expression does not follow the measured variation of the charge fraction. Figure 3 shows the behaviour of the effective velocity with respect to $\alpha(v_c^* = -v_o^P \ln(\eta^+))$; its maximum is situated at $\alpha \approx 30°$, i.e. near the specular angle. This result is consistent with a model proposed by Lee and George [18] in which v_c^* is a function of the experimental parameters α and E_0.

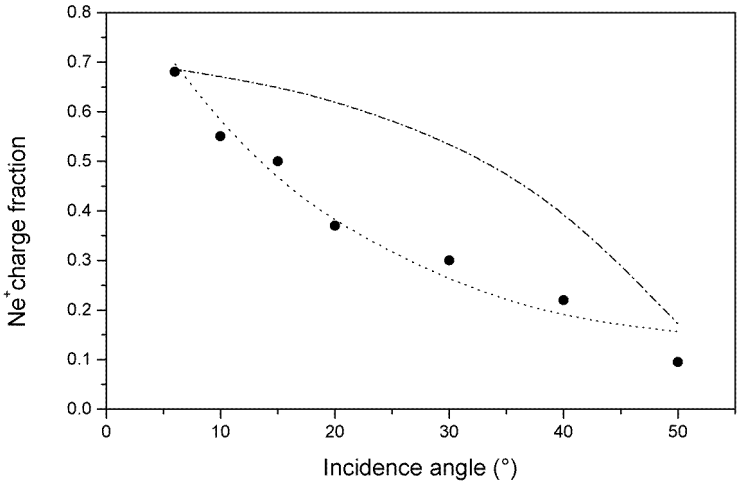

Figure 2. Variation of Ne^+ charge fraction versus incidence angle α ($E_0 = 4$ keV, $\theta = 60°$). ●: experimental values; — · —: Hagstrum model with $v_c = 40\,000$ m s^{-1}; ·····: our model (see text for numerical values).

As in the case of scattering angle variations, this result can be accounted for in terms of depth dependent neutralization with $v_c^* = \lambda D + v_c$, using the D values given by MARLOWE simulations and the above values for $\lambda(1.8 \times 10^{14}$ s$^{-1})$ and $v_c(1.5 \times 10^4$ m s$^{-1})$ (see variations of D in figure 3). The ratio η^+/f_0, equal to the probability f_{ins} of the ion survival inside the solid, decreases from 1 at 6° to 0.55 at 50°. This result differs from those reported by Guillemot *et al* [11] which shows that for 2 keV Ne^+ scattered off the Mg surface the charge fraction η^+ is only dependent on the exit angle regardless of α variation. This can be due on the one hand to the fact that for a primary energy of 2 keV the depth penetration is lower than for 4 keV and on the other hand because the used α range is narrower than that reported here.

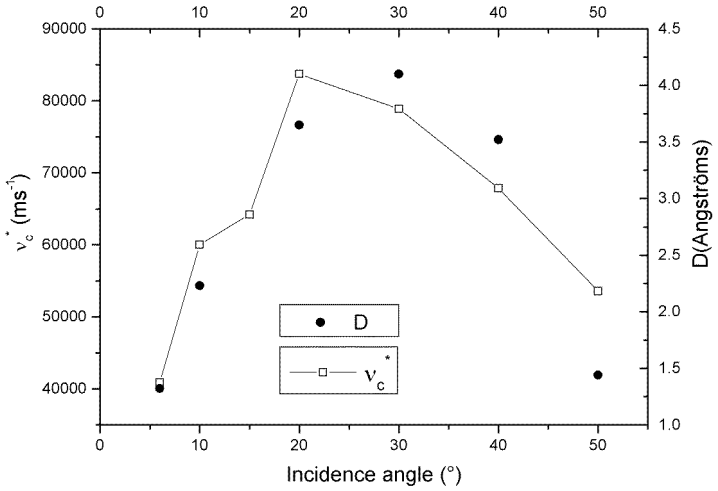

Figure 3. Effective velocity behaviour as a function of the incidence angle. Comparison with the calculated values of the mean depth (D) where close collision occurs ($E_0 = 4$ keV, $\theta = 60^\circ$).

3.4. Charge fractions versus incident energy

The primary energy has an important effect on the parameters governing charge fractions: velocity of incoming and outgoing particles, penetration depth and close encounter conditions. To emphasize this, we present in figure 4 the results of Ne^+ charge fraction measurements obtained as a function of the incident energy at fixed scattering and incidence angles ($\theta = 40^\circ$, $\alpha = 20^\circ$). We can remark that the charge fraction η^+ grows rapidly when E_0 increases between 2 and 10 keV and then becomes almost constant for higher energies. We compared this behaviour with our penetration model and with the simple Hagstrum

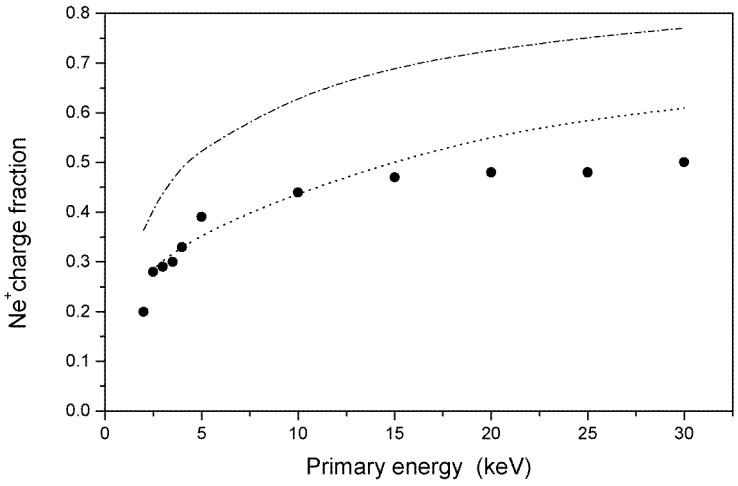

Figure 4. Variation of Ne^+ charge fraction versus primary energy ($\alpha = 20^\circ$, $\theta = 40^\circ$). ●: experimental values; — · —: Hagstrum model with $v_c = 40\,000$ m s^{-1}; ·····: our model (see text for numerical values).

law. Figure 4 shows that our model gives absolute values of charge fractions in reasonable agreement with the experimental results. The discrepancies observed at high energies could be explained by the crudeness of our model assuming a single violent collision to reionize the projectile.

3.5. Doubly ionized Ne^{2+} charge fraction

Figure 5 shows the doubly charged Ne^{2+} ion fraction obtained at grazing incidence, $\alpha = 6^\circ$, versus the scattering angle. For 4 and 9 keV primary energies the Ne^{2+} yield is always lower than the Ne^+ one in the same experimental conditions. According to the electron promotion model, the presence of Ne^{2+} can be explained by the transition of two electrons into the continuum [3, 19] via the highly promoted 4fσ MO during the close collision. Another possibility is the one electron excitation mechanism proposed by Souda *et al* [20], in which an incident Ne^+ ion is excited by the promotion of one electron in the 4fσ which then crosses the surface electronic band, resulting in an irreversible transfer of this electron in the band [21].

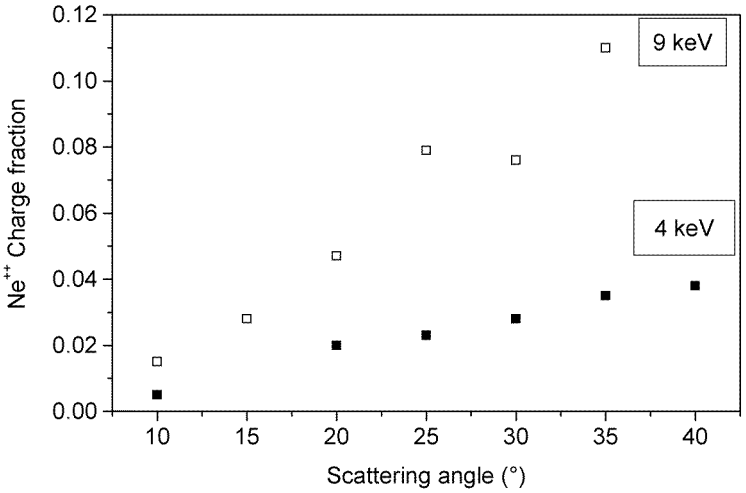

Figure 5. Variation of the Ne^{2+} charge fraction as a function of the scattering angle for two values of the primary energy ($\alpha = 6^\circ$): ■: 4 keV and □: 9 keV.

In a recent paper Ascione *et al* [22] measured the discrete energy loss of Ne^{2+}; their value of 85–87 eV is in agreement with previous results of Wittmaack [23]. This energy loss corresponds to the ionization plus excitation of a surviving Ne^+ in the close collision; this Ne^{2+*} ion decays directly into the Ne^{2+} ground state or through electron capture into Ne^{+**} followed by autoionization (this autoionization is responsible for the low intensity electron line observed at 30.4 eV [24]). This process implies that some of the incoming ions should not be neutralized until the hard collision event; this seems to be likely for primary energy exceeding 5 keV as we will show below. Wittmaack [23] shows a very sharp increase between 1.5 and 4 keV of the relative intensity of back-scattered Ne^{2+} with respect to Ne^+ in the case of collision with an Si surface under normal incidence and the suggested extrapolation indicates a ratio Ne^{2+}/Ne^+ of unity at 7 keV. Our results for $\alpha = 6^\circ$ and $\theta = 40^\circ$ give a ratio of 0.08 and 0.18 at 4 and 9 keV respectively.

4. Electron spectra

4.1. Spectrum features

Electron spectra (figure 6) are very similar to those already reported by different authors for Ne^+ scattering on Mg and Al surfaces [3, 5, 25]. The main features superimposed on the continuum are the quasi-atomic Auger spectrum (LMM transitions) from silicon [26, 27] in the range 75–95 eV and the autoionizing lines from neon doubly excited states ($2p^4nl\ n'l'$) in the range 15–30 eV [28]. The autoionization lines from Ne^{**} represent only a very small part of the total electron production but they are the most direct proof of the important role of the electron promotion mechanism in the close collision.

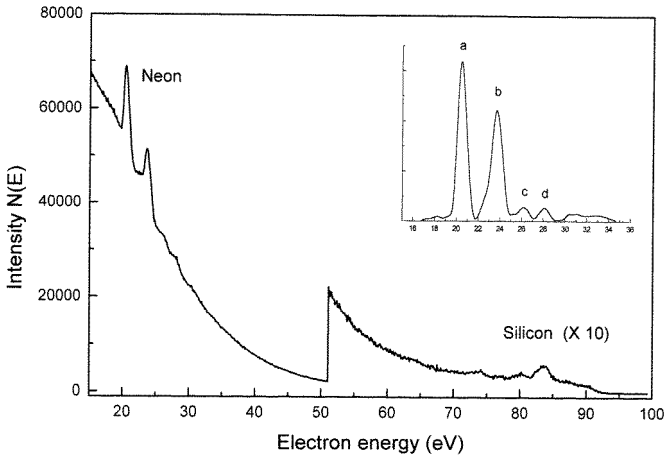

Figure 6. Electron spectrum showing the autoionizing lines of neon and the silicon Auger lines. $E_0 = 4$ keV, $\alpha = 10^\circ$ (in the inset: neon spectrum after background subtraction).

Starting from the gas phase electron or ion collision data [29, 30], many identifications have been made in the case of collisions of Ne with surfaces [6, 24, 28, 31]. The two most important lines at 20.45 (a) and 23.70 eV (b) are attributed to the $2p^4(^3P)3s^2$ and $2p^4(^1D)3s^2$ Ne^{**} states decaying in vacuum into Ne^+ $2p^5$. At higher energies we observe two smaller peaks which can be assigned to $2p^4(^1D)[3s3p(^3P)]^3F$ (26.2 eV) (c) and $2p^4(^1D)[3s3p(^1P)]^1P,D,F$ (28.1 eV) (d). These lines correspond to those labelled 1, 3, 4, 6 by Gallon and Nixon [24].

The first observation we can make is, as in the case of metal surfaces, the strong excitation of the ^3P core state and the low number of observed lines in contrast to the situation in gas phase collisions [30]. The excited states with ionization potential lower than the work function of the surface are destroyed before autoionization by resonant ionization. Unlike the case in gas phase collisions, the ^3P core autoionizing line is always the strongest; to explain this phenomenon different core rearrangement processes in the outgoing path of the excited atom have been proposed [3, 4, 6]. Indeed, during the close collision the promotion of two 2p electrons via the $4f\sigma$ MO can only produce singlet core states. The core rearrangements result from electron exchange processes between the receding Ne^{**} and the surface, producing triplet core states with a high probability. The rearrangement mechanisms are efficient only if the excited atoms spend a long time in the vicinity of the surface as confirmed by varying the experimental parameters (see below).

4.2. Line intensity

After subtraction of a smooth background, we have measured the variation of the two prominent lines as functions of the primary energy and incidence angle of the projectile (figure 7). One can observe a rapid increase of the total $^3P + {}^1D$ intensity between 1 and 6 keV. A similar behaviour was observed for collisions with Mg and Al surfaces [3, 4] but with a maximum of intensity located at lower energy.

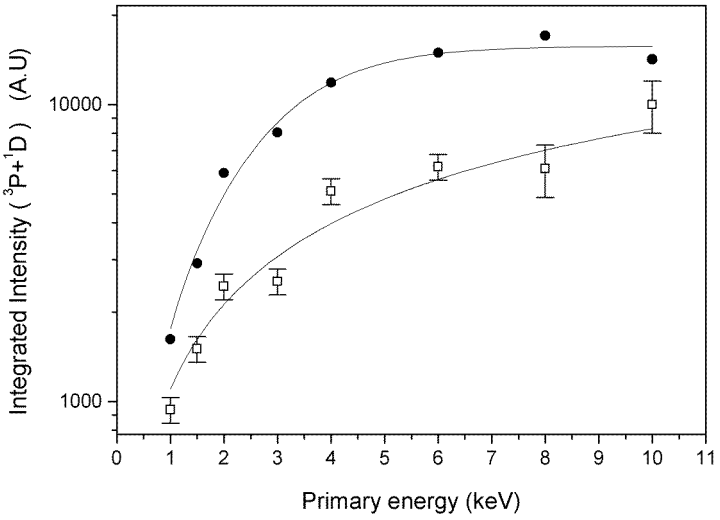

Figure 7. Ne doubly excited state production efficiency as a function of the primary energy for two incidence angles. ●: $\alpha = 10^\circ$, □: $\alpha = 20^\circ$.

4.3. Core conversion efficiency

The core conversion can be characterized by the conversion efficiency ε_{con} defined as the ratio of the ^3P line intensity over the sum of ^3P and ^1D intensities. All the proposed core rearrangement mechanisms involve electron exchange between Ne doubly excited states and the surface. The efficiency should depend on the interaction time of the Ne atom with the surface after the close collision, therefore it is expected that the conversion efficiency depends on the perpendicular velocity of the scattered particle on the way out. We determined this efficiency under different experimental conditions: as a function of the primary energy and of the incidence angle.

Figure 8 shows the measured efficiency as a function of the Ne^+ beam primary energy E_0 at several incidence angles. This efficiency is lower than that measured for Mg and Al surfaces in similar conditions; measurements of ε_{con} by Bonanno *et al* [32] at a collision energy of 700 eV indicate a gradual decrease from Mg to Al and to Si; for Si they obtain a value of 0.72 consistent with ours, having in mind that the conversion efficiency increases with decreasing incident energy.

For a given incidence angle, the conversion efficiency presents a rapid decrease between 1 and 5 keV, followed by an asymptotic limit of 0.55 independent of α. From these observations we can conclude that for incident energies lower than 5 keV the variation

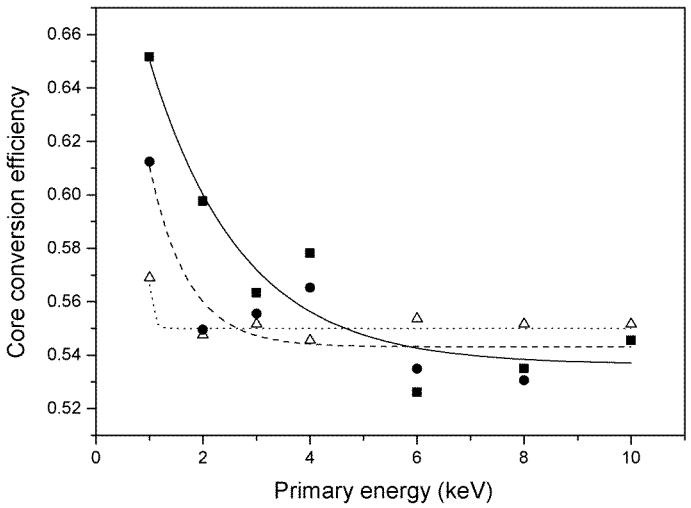

Figure 8. Core conversion efficiency ($^1D \rightarrow {}^3P$) versus primary energy at several incidence angles (△) $\alpha = 6^\circ$, (●) $\alpha = 10^\circ$, (■) $\alpha = 20^\circ$.

of conversion efficiency with E_0 agrees with the rearrangement mechanisms along the outgoing trajectory. But for higher energies, the asymptotic behaviour of ε_{con} suggests that part of the ^3P creation is not due to core conversion of the ^1D state. Indeed, there are two possibilities for a more *direct* creation of the triplet core states: either some ions neutralized in the incoming path are in excited states at the time of the violent collision or some incident ions survive neutralization until the close collision, this is more probable as the incident energy increases. In both situations [20, 21], during the close encounter the 2p vacancy may be in the 4fσ or in the 3dπ orbital. In the latter case the promotion of two electrons via 4fσ gives after the interaction a doubly excited neon ion or a triply excited neutral. In the case of a doubly excited ion Ne^{+**} ($2p^3$ *nl n′l′*), an autoionizing state with a triplet or a singlet core could be produced through Auger or resonant capture with the same probability [21]. Doubly excited ions can directly autoionize into doubly charged Ne ions; this process has been confirmed by the observation of a very small line at 30.4 eV in the autoionization spectra of Ne on Al and Si [24, 33] and by the value of the inelastic collisional energy loss of Ne^{2+} ions produced in Ne^+–Al and Si collisions [22, 23]. When the projectile becomes more energetic, these quasi-direct processes compensate the loss of efficiency of the core rearrangement processes due to the increase of the perpendicular velocity.

At incident energies below 4 keV, ε_{con} increases clearly with α (figure 9); this behaviour has also been reported by Xu *et al* [33] in the case of interaction of Ne^+ ions with Al and by Lacombe *et al* [13] for Ne^+ on Mg. Xu *et al* calculated the excitation cross section of an Ne projectile in a single binary collision with a target Al atom as a function of the normal velocity of the receding particle. Their calculations show that the average normal velocity of the receding Ne decreases monotonically with the incidence angle α for a given primary energy. This can be confirmed by our previous experimental results [34] which show that the angular distribution of the scattered Ne^+ ions exhibit a maximum for an exit angle, $\beta = \theta - \alpha$, between 13 and 15°, almost independent of the value of the incidence

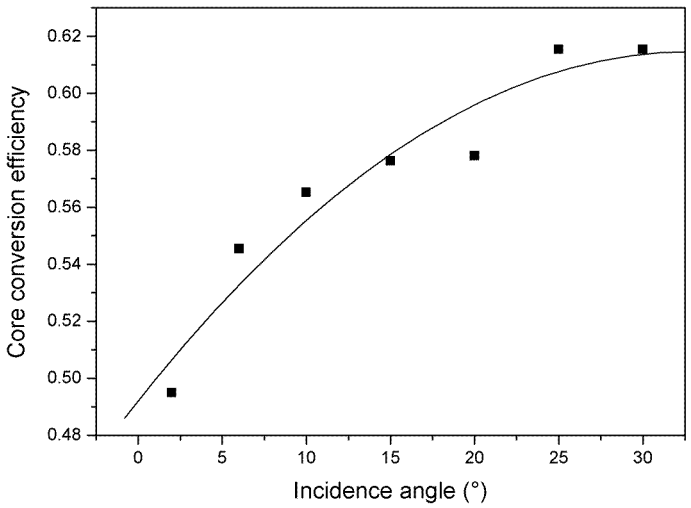

Figure 9. Core conversion efficiency ($^1D \rightarrow {}^3P$) versus incidence angle ($E_0 = 4$ keV).

angle. Moreover, a similar distribution was obtained in a simulation performed by T Vu Ngoc [35]. As the average value of the exit angle does not depend on the α value, then the average value of the normal velocity decreases with α because for a given β value the energy of the receding particle decreases (larger scattering angle). For instance, at 4 keV primary energy and at $\beta = 14^\circ$, the normal velocity decreases from 49 280 to 40 590 m s^{-1} when α increases from 2° to 30°. A decrease of the normal velocity corresponds to an increase of the mean interaction time with the surface in the outgoing path and thus to an increase of the conversion efficiency.

4.4. Line profile analysis

The autoionization electrons are ejected from an emitter moving in the laboratory frame, hence the shape and the energy of the observed lines are modified by a kinematic Doppler effect [36]. The analysis of the line profiles can give information about the angular distribution of the emitters [37, 38]. Under our experimental conditions, an observation angle of 90°, the electron spectra are asymmetric and shifted due to the presence of the surface which breaks the azimuthal symmetry of emitters, so the shape and width of the measured lines are sensitive to the emitter polar and azimuthal distribution. In all measurements the ^3P peak is narrower than the ^1D one; both have a high energy wing steeper than the low energy one (figure 10). The observed line profiles can be reproduced with emitter polar distributions broader for ^1D than for ^3P (see inset of figure 10), these distributions being very similar to those obtained by the Orsay group [4]. This result is consistent with core conversion mechanisms in the vicinity of the surface, the atoms in ^3P states being on average scattered closer to the surface. Moreover, we observed that the low energy side of the peaks is well reproduced only with emitters having a narrow azimuthal distribution around the collision plane, as recently confirmed by the simulation done by T Vu Ngoc [35].

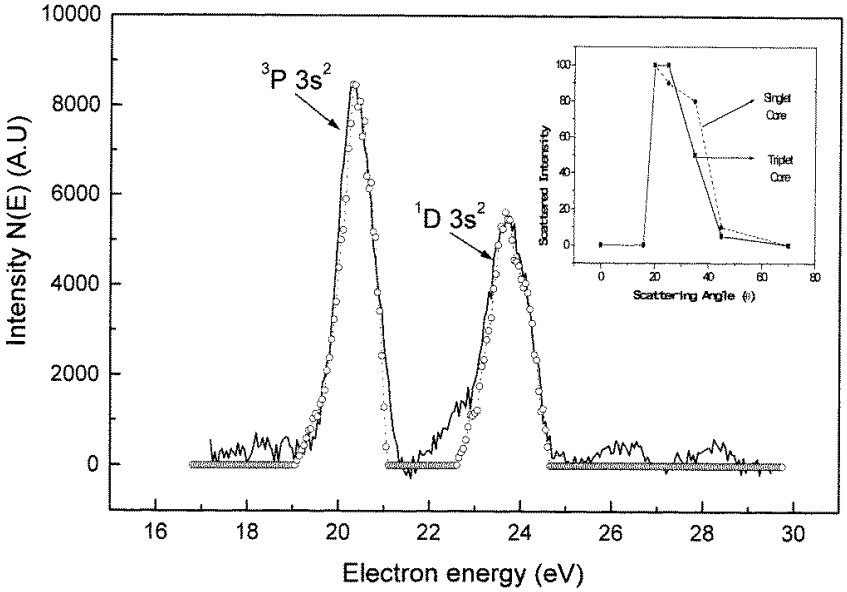

Figure 10. Reconstitution of ^{3}P and ^{1}D peak profile of Ne lines ($E_0 = 4$ keV, $\alpha = 6°$). Experiment: solid line, ○: simulation. In the inset, emitter angular distributions used in the simulation of Doppler profiles, ■: ^{3}P, ●: ^{1}D.

5. Conclusion

We measured the Ne^+ charge fraction in scattering of Ne^+ on an a:Si surface as a function of the incidence and scattering angles and of the primary energy. The results are very similar to those for Mg and Al surfaces because the exchange mechanisms are almost the same: Auger neutralization on the way in and out and reionization in the close collision with one atom of the target; for these interactions the gap of Si plays no role for neon incident ions. To account for these results we proposed a model which highlights the role of the penetration of the projectile inside the bulk material. This model allows us to generalize the model proposed by Hagstrum in the case of surface Auger neutralization.

We also measured the energy distributions of the electrons emitted during these collisions; the autoionization lines from neon superimposed on the continuum of the electrons are the proof of the role of electron promotion mechanisms in the Ne–Si close collision. The variations of the $^1D \rightarrow {}^3P$ conversion efficiency as a function of the primary energy and the incidence angle show a novel aspect concerning the conversion efficiency. The nearly constant value observed when the projectile energy exceeds 5 keV cannot be explained by the core rearrangement mechanisms and is then mainly ascribed to a direct creation of Ne^{**} states from ions escaping neutralization in the incoming trajectory.

References

[1] Hagstrum H D 1954 *Phys. Rev.* **96** 336
Hagstrum H D, Petrie P and Chaban E E 1988 *Phys. Rev.* B **38** 10 264
[2] Mouhammad S, Benoit-Cattin P, Benazeth C, Benazeth N, Cafarelli P, Richard-Viard M and Ziesel J P 1997 *Nucl. Instrum. Methods* B **125** 297
[3] Zampieri G, Meier F and Baragiola R 1984 *Phys. Rev.* A **29**

[4] Guillemot L, Lacombe S, Maazouz M, Sanchez E and Esaulov V A 1996 *Surf. Sci.* **356** 92 and references therein
Guillemot L, Lacombe S, Vu Ngoc T, Esaulov V A, Sanchez E, Bandurin Y A, Dashenko A I and Drobnich V G 1996 *Surf. Sci.* **365** 353
[5] Pepper S V and Aron P 1986 *Surf. Sci.* **169** 14
[6] Xu F, Baragiola R A, Bonanno A, Zoccali P, Camarca M and Oliva A 1994 *Phys. Rev. Lett.* **72** 4041
[7] Pepper S V 1986 *Surf. Sci.* **169** 39
[8] Esaulov V A 1994 *J. Phys.: Condens. Matter* **6** L699
[9] Benazeth C, Benoit-Cattin P, Cafarelli P, Reynes P, Ziesel J P and Benazeth N 1994 *Nucl. Instrum. Methods* B **94** 581
[10] Barat M and Lichten W 1972 *Phys. Rev.* A **6** 211
Souda R, Yamamoto K, Hayami W, Aizawa T and Ishizawa Y 1995 *Surf. Sci.* **343** 104
[11] Guillemot L, Lacombe S, Huels M, Vu Ngoc T and Esaulov V A 1994 *Nucl. Instrum. Methods* B **90** 270
[12] Rabalais J W, Chen J, Kumar R and Narayana M 1985 *J. Chem. Phys.* **83** 6489
[13] Lacombe S, Esaulov V A, Guillemot L, Grizzi O, Maazouz M, Mandarino N and Vu Ngoc T 1995 *J. Phys.: Condens. Matter* **7** L261
[14] Verhey L K, Poelsema B and Boers A L 1975 *Radiat. Eff.* **27** 47
Verhey L K, Poelsema B and Boers A L 1976 *Nucl. Instrum. Methods* **132** 565
[15] Luitjens S B, Algra A L, Suurmeijer E P and Boers A L 1980 *Surf. Sci.* **99** 631
[16] MacDonald R J, O'Connor D J and Higginbottom P R 1984 *Nucl. Instrum. Methods* B **2** 418
O'Connor D J, Shen Y G, Wilson J M and MacDonald R J 1988 *Surf. Sci.* **197** 277
[17] Robinson M T and Torrens I M 1974 *Phys. Rev.* B **9** 5008
[18] Lee H W and George T F 1985 *Surf. Sci.* **159** 214
[19] Hird B, Armstrong R A and Gautier P 1994 *Phys. Rev.* A **49** 1107
[20] Souda R, Yamamoto K, Hayami W, Aizawa T and Ishizawa Y 1995 *Phys. Rev. Lett.* **75** 3552
[21] Souda R 1997 *Int. J. Mod. Phys.* B **11** 685
[22] Ascione F, Manico G, Bonanno A, Oliva A and Xu F 1997 *Surf. Sci.* **394** L145
[23] Wittmaack K 1996 *Surf. Sci.* **345** 110
[24] Gallon T E and Nixon A P 1992 *J. Phys.: Condens. Matter* **4** 9761
[25] Grizzi O, Shi M, Bu H and Rabalais J W 1990 *Phys. Rev.* B **41** 4789
[26] Mischler J and Benazeth N 1986 *Scanning Electron Microsc.* **2** 351
[27] Valeri S 1993 *Surf. Sci. Rep.* **17** 85
[28] Zampieri G and Baragiola R A 1982 *Surf. Sci.* **114** L15
[29] Spence D 1981 *J. Phys. B: At. Mol. Phys.* **14** 129
[30] Olsen J O and Andersen N 1977 *J. Phys. B: At. Mol. Phys.* **10** 101
[31] Blum V, Brugger A, Nixon A P and Gallon T E 1994 *J. Phys.: Condens. Matter* **6** 9677
[32] Bonanno A, Zoccali P and Xu F 1994 *Phys. Rev.* B **50** 18 525
[33] Xu F, Mandarino N, Oliva A, Zoccali P, Camarca M and Bonanno A 1994 *Phys. Rev.* A **50** 4040
[34] Benazeth C, Benazeth N, Benoit-Cattin P, Cafarelli P, Mouhammad S and Ziesel J P 1995 *Surf. Sci.* **343** 240
[35] Vu Ngoc T 1997 *Surf. Sci.* **371** 111
[36] Gleizes A, Benoit-Cattin P, Bordenave-Montesquieu A and Merchez H 1976 *J. Phys. B: At. Mol. Phys.* **9** 473
[37] Pepper S V 1986 *Surf. Sci.* **169** 39
[38] Esaulov V A 1995 *J. Phys.: Condens. Matter* **7** 5303